
Proceedings Paper:
Mendham, E.M., Rigby, S.E. orcid.org/0000-0001-6844-3797, Farrimond, D.G. et al. (4 more authors) (2025) Numerical investigation of blast loading from cube shape explosive charges. In: Proceedings of the 27th International Symposium on Military Aspects of Blast and Shock (MABS27). 27th International Symposium on Military Aspects of Blast and Shock (MABS27), 05-10 Oct 2025, Colmar, France. Military Aspects of Blast and Shock (MABS).

NUMERICAL INVESTIGATION OF BLAST LOADING FROM CUBE SHAPE EXPLOSIVE CHARGES

Ella M Mendham[1], Samuel E Rigby[1,2], Dain G Farrimond[1], Andrew Tyas[1,3], Peter McDonald[4], Andrew Nicholson[4], Genevieve Pezzola[5]

[1]School of Mechanical, Aerospace & Civil Engineering, University of Sheffield, Mappin Street, Sheffield, S1 3JD, UK;
[2]ARUP Resilience, Security and Risk, Manchester, UK;
[3] Blastech Ltd., The Innovation Centre, 217 Portobello, Sheffield, S1 4DP, UK;
[4] Viper Applied Science, Aberdour, UK;
[5] The U S Army Corps of Engineers, Engineer Research & Development Center, 3909 Halls Ferry Rd, Vicksburg, MS 39180, USA.

Key words: Numerical modelling, Cube charge, CFD, Viper Blast

ABSTRACT

Accurate and rapid quantification of blast loading is essential to ensure infrastructure resilience against explosions. There is significant literature on the assessment of the blast output from (hemi-)spherical charges, and it is generally accepted that simplified empirical methods and high-fidelity numerical solvers can accurately quantify the loading from these charges. Many explosions, accidental or otherwise, are not the result of such idealised charge shapes, and therefore the associated loading may significantly differ from those predicted by modelling. This work investigates the accuracy of using the CFD code Viper Blast as a tool for modelling cube-shaped charges in the far field. The models are compared to well-controlled experimental data from previous work using 250g PE4 charges at a range of standoff distances. Cube charges are shown to exhibit a significant subsequent shock, equal in magnitude to the primary shock in some instances. It is shown that Viper Blast is able to model this behaviour with sufficient accuracy, however the results are highly mesh dependent and sensitive to the exact choice of equation of state parameters used to represent the explosive. The modelling work indicates that loading features which persist well into the far field are governed by complex early-stage processes which are not present in commensurate models with hemispherical charges. This highlights the need to accurately model detonation and immediate post-detonation behaviour in numerical simulations in order to represent far field blast loading of non-spherical explosive charges.

BACKGROUND

Significant research has been carried out in order to quantify the blast response of (hemi-)spherical charges, using both experimental and numerical methods [1-3]. However, whilst there has been some investigation into the blast parameters of non-(hemi-)spherical charges, this has not been done to the same degree, and as such predictors based on the Kingery Bulmash method [1] like the Unified Facilities Criteria (UFC) 3-340-02 [4] and *Load_Blast_Enhanced in the commercial finite element code LS-DYNA [5] may not be valid for these shapes.

This paper follows on from previous work by the current authors [6], wherein it was shown that a gauge aligned with the flat face of a cube charge will exhibit a significant subsequent shock which follows the primary shock. For further afield charges (7.4 and 11.9 m/kg$^{1/3}$) the primary shock was also lower than expected from a hemispherical charge of the same mass. The work also compares the cube data with a well-recognised predictive tool - UFC predictions of an equivalent mass hemisphere, which does not include the subsequent peak and its effects.

This paper will present a comparison of experimental data from Mendham et al [6] with Viper Blast (henceforth referred to as Viper) [7] models of the same experimental setup. Viper is a GPU based Computational Fluid Dynamics (CFD) solver specifically designed to simulate blast loading from high explosives and is capable of accounting for wave interactions. Viper was chosen for this analysis due it its accessible user interface and high speeds [8] compared to other modelling software such as blastFoam [9] and Autodyn [10]. It has also been thoroughly validated against hemispherical air-blast tests [8, 11].

Studies have shown that charge geometry influences shock propagation [12, 13], so whilst a hemispherical charge detonated in free air will result in a blast wave that propagates out equally in all directions, this is not the case for non-(hemi-)spherical charges. For cylindrical and cube charges, it has been shown that overpressure is magnified in areas of highest presented surface area [14-20]. Vorobiev and Ford [20] also observed a distinct additional shock for the gauge oriented toward the flat face of a C4 cuboid charge with explosive yield of 992 kg TNT at a scaled distance of 20m/kg$^{1/3}$, where the magnitude of the additional shock significantly outweighed that of the primary shock. In a cuboidal charge, as the hemispherical detonation wave expands, it meets the boundary of the flat faces first, whilst continuing to propagate through the mass held in the corners and edges of the cube. When the detonation wave reaches this boundary, it forms an additional wave. This behaviour is not observed in (hemi-)spherical charges.

Additional waves from cuboid charges have been observed in a variety of sources, however there is as yet no confirmation as to whether these features can be captured by numerical modelling. This paper aims to assess the accuracy of Viper Blast as a tool to model blast behaviour from cube charges.

METHODOLOGY

Experimental methodology

Nine experiments were conducted at The University of Sheffield Blast and Impact laboratory. 250g PE4 was formed into 1:1:1 (L:W:H) cubes of 55.5mm side length using 3D printed charge moulds to preserve the sharpness of the corners and edges of the charge. An example charge is shown in Figure 1. All charges were orientated with opposing faces orthogonal to the reflecting walls.

Figure 1: Anvil mounted 1:1:1 PE4 cube charge

The tests were carried out on a flat concrete ground slab, inset with a channel which was filled with sand after positioning the charge atop a steel anvil. The anvil has a centrally drilled hole, housing the detonator and associated cabling. This ensured the base of the charge was flush with the ground level, and that the charge could be bottom detonated. The sand was smoothed, and the concrete slab was swept before each test to ensure an unobstructed surface for the blast wave to propagate over. Two 4m high blockwork walls were positioned 10m apart at either side of the slab (shown in Figure 2), sufficiently tall and wide that no clearing waves [21] would arrive within the positive phase and therefore the reflecting surface could be assumed as effectively semi-infinite. Piezoresistive pressure gauges, used to take pressure measurements, were mounted on steel plates on the front of the walls at ground level.

Further detail on the specifics of testing can be found in Mendham et al [6].

Figure 2: Concrete test pad with reflecting walls on the far left and right, with sand channel running between.

Computational Modelling Methodology

The numerical model comprised a 0.6x0.6x0.3m domain with the charge placed centrally at ground level. A cell size of 1mm was used to model the first stages of detonation. It is key to model the initial stages of detonation with the smallest feasible cell size in order to capture any features that develop during the detonation stage [22]. This can then be remapped into a larger domain with a larger cell size. In this case, quarter symmetry was used in order to minimise domain size, allowing for increased resolution. Note that 1D symmetry, whilst available in Viper, was not used on account of the shape of the charge.

The detonation and initial propagation was modelled out to 0.3m, utilising a full domain, at which point the model was remapped into a quarter symmetrical domain, utilising only a quarter of the charge and its initial detonation in a larger domain. The domain was sized as follows: Y=3m, Z=3m based on a domain size analysis, with the X domain equal to the standoff distance of the specific tests (ranging from 2-8m).

Figure 3 shows the initial full domain before (3a) and after (3b) detonation, and the following Quarter Symmetry (QS) domain with the detonation remapped in (3c). The QS domain utilised a cell size of 7.5mm, as determined by a mesh sensitivity analysis. The gauges used to measure the pressure history were positioned at floor level and inset 1mm from the X boundary in order to measure the pressure at the specified standoff distance. This allowed the pressure to be captured without any interference caused by the boundary, whilst still allowing the boundary to act as a reflecting surface, mirroring that of the wall in the physical tests.

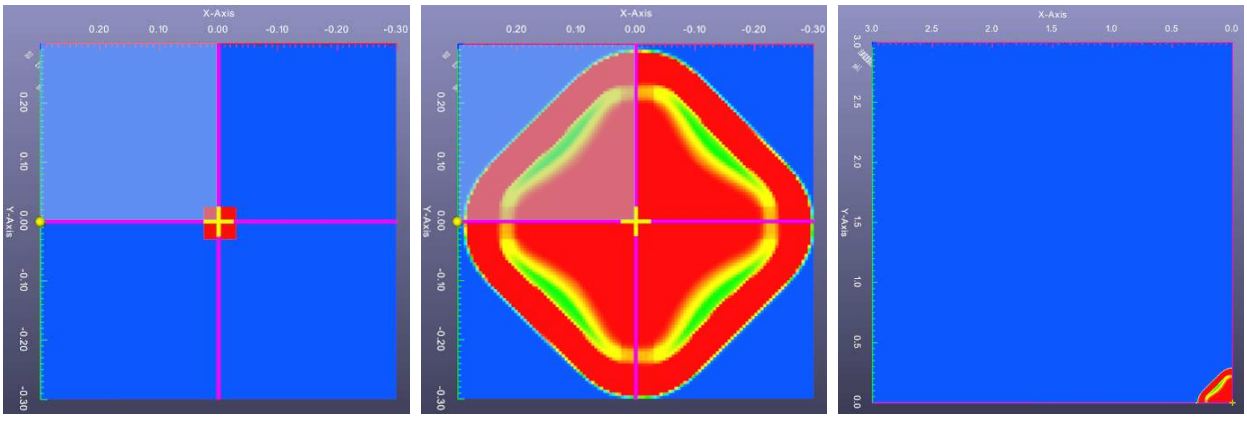

(a) (b) (c)

Figure 3: Showing the progression of a C4 Viper model. From left to right – (a) the initial domain with charge, (b) the initial domain post detonation and initial expansion, (c) the quarter symmetry domain with the detonated charge remapped in. The highlighted upper left quadrant of (a) and (b) illustrates the quarter symmetry used in (c).

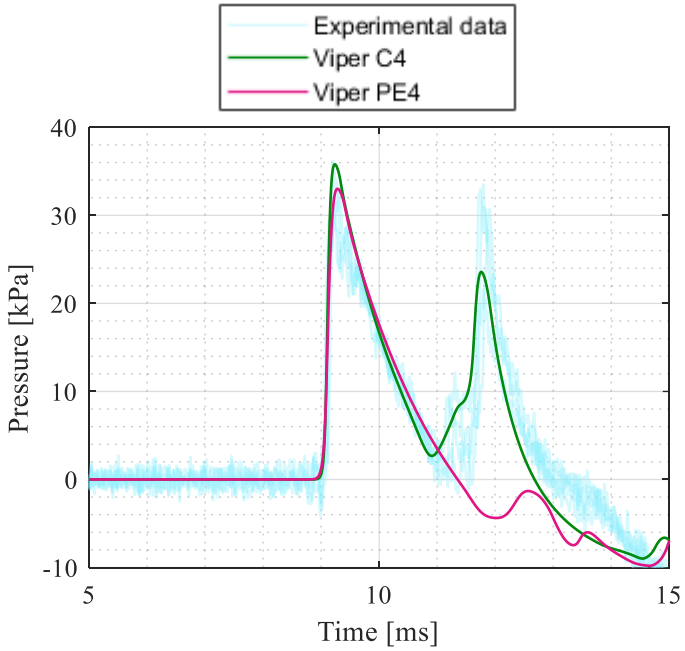

Figure 4: Comparison of Viper models using the inbuilt PE4 and C4 parameters, with experimental data.

Figure 4 shows preliminary modelling carried out using Viper's inbuilt PE4 and C4 parameters. As can be seen, the PE4 model does not capture the subsequent shock seen in the experimental data. This is a result of the optimisation of Viper's PE4 parameters, carried out using a genetic algorithm based on data from Netherton et al [23]. This data set features only hemispheres and cylinders, and its applicability for cuboidal charges has not yet been investigated.

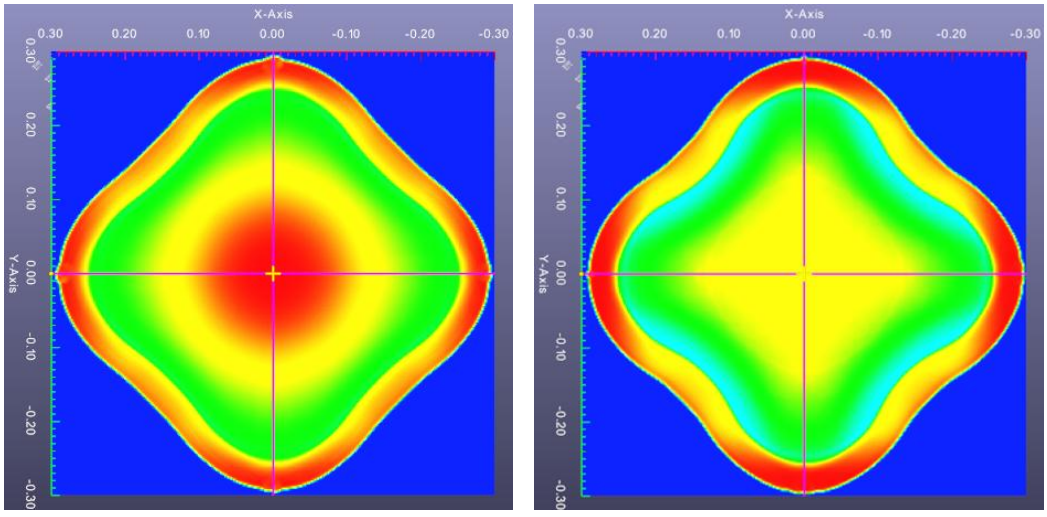

(a) (b)

Figure 5: Viper Blast models of the initial detonation and initial expansion of a cube charge modelled using inbuilt parameters for PE4 (a) and C4 (b).

Figures 5a and 5b show the domains post initial detonation and expansion of a PE4 and C4 cube respectively. It is clear that, whilst the primary shock is captured well by both

materials (as in Figure 4), the coalescence of waves in the centre of the charge has formed very differently. The PE4 (Figure 5a) has formed into a circle, akin to the behaviour of a (hemi-)spherical secondary shock [24], but the C4 (Figure 5b) has formed a distinct square, similar to that of the shape of the primary shockwave. This distinction, belived to be a direct result of the PE4 parameters development using experimental data from hemispheres and cylinders, is a significant contributor to the difference in model response and capture of the subsequent shock. Experimentally, C4 exhibits similar behaviours to PE4 [25], with reliable Jones-Wilkins-Lee (JWL) [26] parameters evaluated through CYLEX trials [27]. Viper's inbuilt C4 parameters are based on these Lawrence Livermore values, and whilst the applicability of C4 parameters for modelling cuboids has also not been investigated, Figure 4 shows C4 offers a far more accurate representation of the experimental data. The C4 parameters are therefore used in place of PE4 for the Viper models.

Viper calculates cuboid charge height using the charge width, length and the density, so the density and therefore charge height was adjusted slightly to match the experimental tests. Viper is capable of modelling detonations using ideal gas or JWL methods, however JWL was used here as it replicates the expansion of the detonation products more accurately [11], particularly in the near-field, which will likely be key for accurately capturing the additional loading features seen from cube charges since these are assumed to develop during detonation and early stages of expansion.

Data extraction methodology

The experimental data was converted from voltage to pressure, then filtered on a case-by-case basis using band and low pass filters to remove background noise, whilst maintaining the key features of the trace, (typically located between 0 and 0.2Hz). Due to the complexity of the waveform casued by the additional shock, locations of arrival time and peak pressure for the primary and additonal shocks was manually extracted via a purpose-written MatLab script. The end of the postive phase was calculated using the point of maximum impulse, which, due to its objectivity, was automatically extracted rather than manually extracted. These 3 points were used to calculate the arrival time and peak pressure of the primary and additional shocks, and the impulse and positive phase duration of the whole waveform. This process was carried out for both experimental data and Viper models alike. Manual selection of points, whilst more cumbersome than fully automated extraction, is crucial here where the waveforms are more complex and may not fit a perfect Friedlander curve [28-30].

RESULTS

Some of the Viper models in this section have been time adjusted so that the arrival time and peak pressure locations of the Viper match that of the experimental data in order to facilitate qualitative analysis. In all cases this was no more than +0.3ms, with Viper arriving earlier than the experiment. The aim of this adjustment was not to perfectly align the primary shock arrival, but align as many key features (arrival times and pressure peaks) as possible.

Figures 6-13 show the pressure and impulse vs time at varying scaled distances (3-11.9m/kg$^{1/3}$). Generally, Viper presents very reasonable predictions of the behaviour of a cube charge at the range of scaled distances discussed herein, especially for the primary shock. Viper's predictions of the shape of the pressure time curves are generally very accurate, capturing the initial rise and decrease in pressure before the subsequent shock remarkably well for all observed scaled distances.

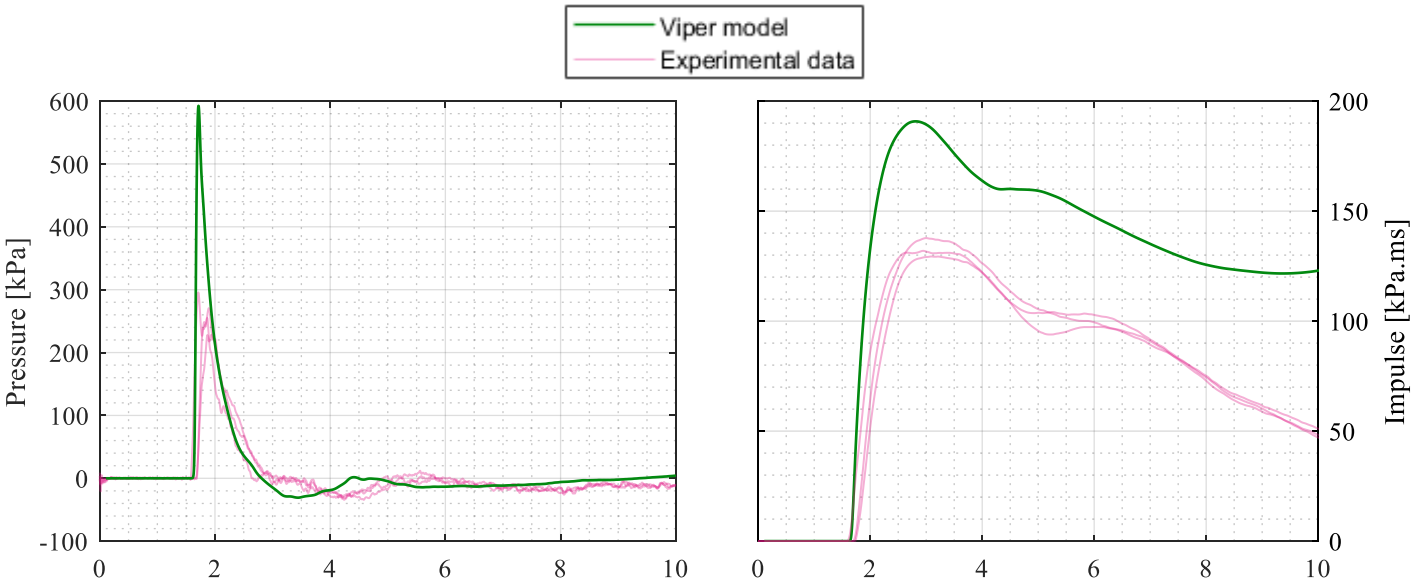

Figure 6: Viper Blast and experimental measurements of Pressure (left) and Impulse (right) vs Time for a cube charge at 2m standoff (3m/kg$^{1/3}$)

Figure 6 shows the pressure-time and impulse-time plots at the smallest tested scaled distance – 3m/kg$^{1/3}$. It shows that Viper overpredicts the peak pressure by almost double (~280kPa vs ~600kPa). However, the general shape of the curve matches that of the experimental data well, with the drop in pressure post peak and end of the positive phase appearing very similar. The impulse time shown in Figure 6 follows a similar pattern: a significant overprediction but the model curve follows a very similar shape to the experimental data, capturing the time of the rise and falls in impulse very well. The experimental data appears to flatten out at ~250-300kPa rather than forming the "usual" sharp peak [31, 32]. The cause of this is possibly spurious gauge response as a result of the blast wave not being planar at the point where it meets the gauge.

Particularly notable in Figures 7-10 is the slight jump in pressure before the arrival of the subsequent shock. This is assumed to be another wave which eventually coalesces with the subsequent shock and is hence not present in traces >10.4m/kg$^{1/3}$. The magnitude of this rise is accurately captured by the Viper models, albeit occurring slightly earlier than in the experimental data. Viper appears to smooth this additional shock (especially visible in Figures 9 and 10) quite significantly, to the point where the drop in pressure before the arrival of the subsequent shock is not captured. This is suspected to be a result of the mesh size, with the effect of rounding the peaks and troughs in pressure [33, 34] if not fine enough. The mesh size used for these models was the finest possible with the available processing power, in this case an Nvidia GeForce RTX 4090 GPU.

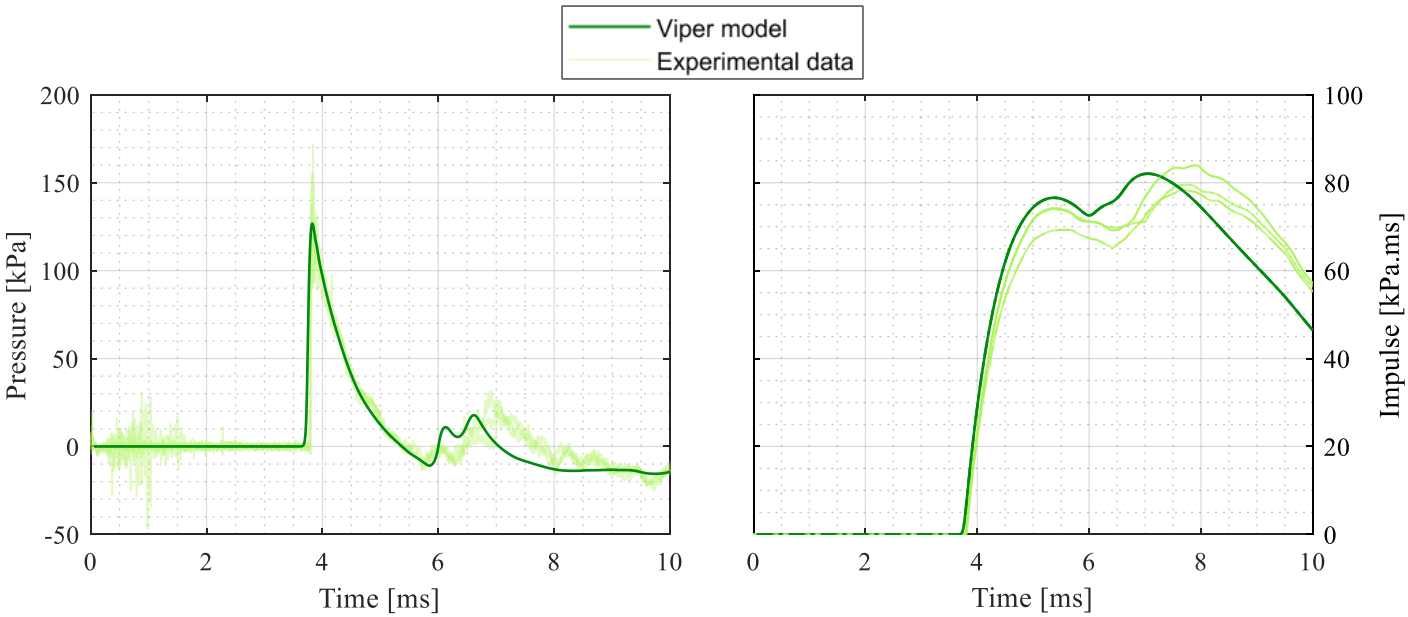

Figure 7: Viper Blast and experimental measurements of Pressure (left) and Impulse (right) vs Time for a cube charge at 3m standoff (4.5m/kg$^{1/3}$)

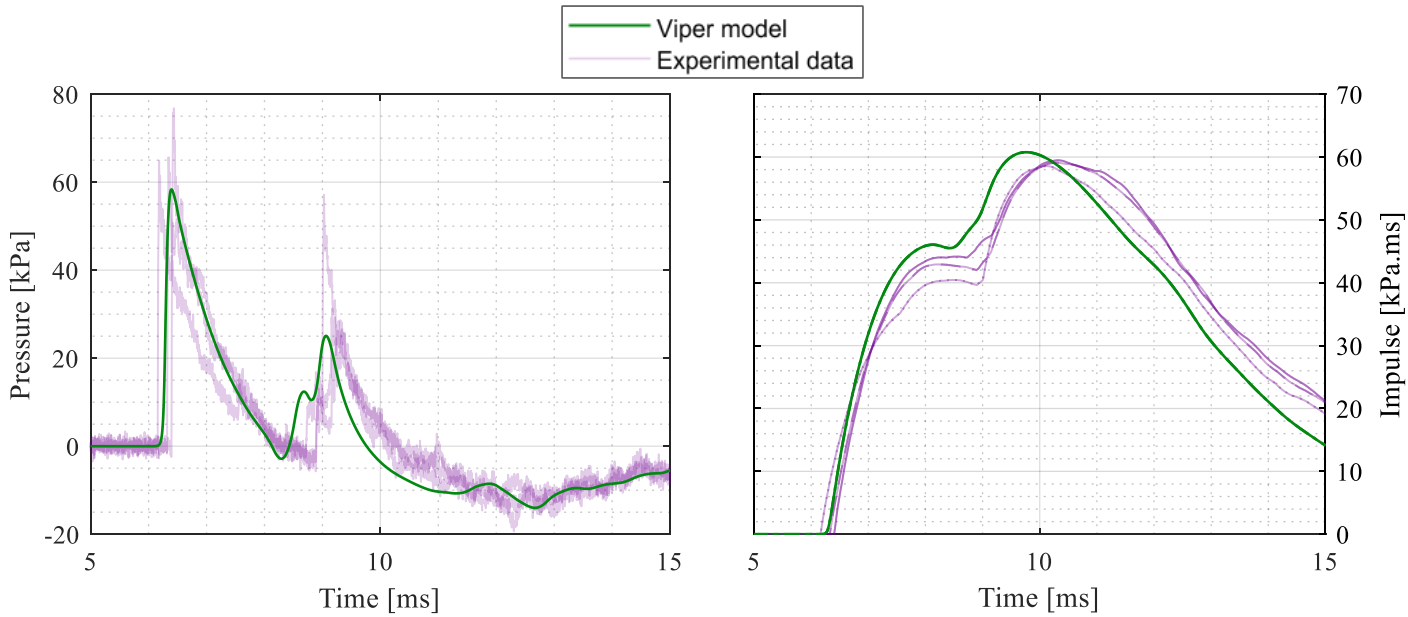

Figure 8: Viper Blast and experimental measurements of Pressure (left) and Impulse (right) vs Time for a cube charge at 3m standoff (5.9m/kg$^{1/3}$)

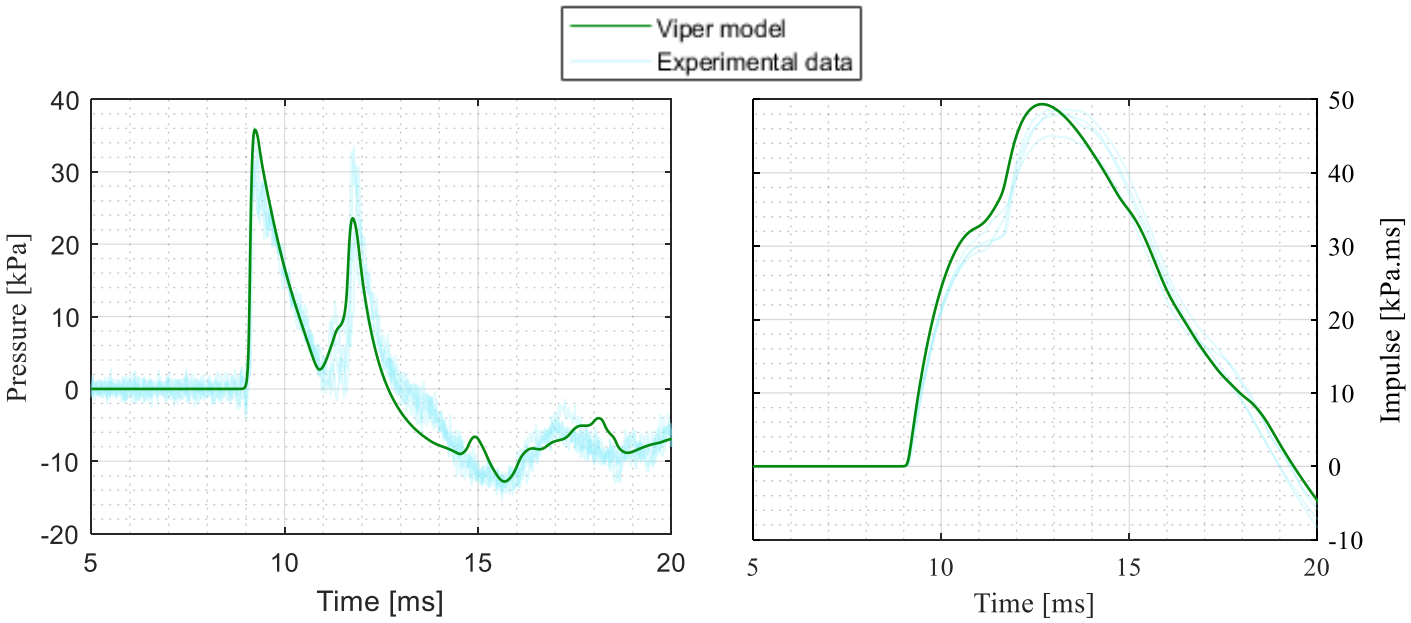

Figure 9: Viper Blast and experimental measurements of Pressure (left) and Impulse (right) vs Time for a cube charge at 5m standoff (7.4m/kg$^{1/3}$)

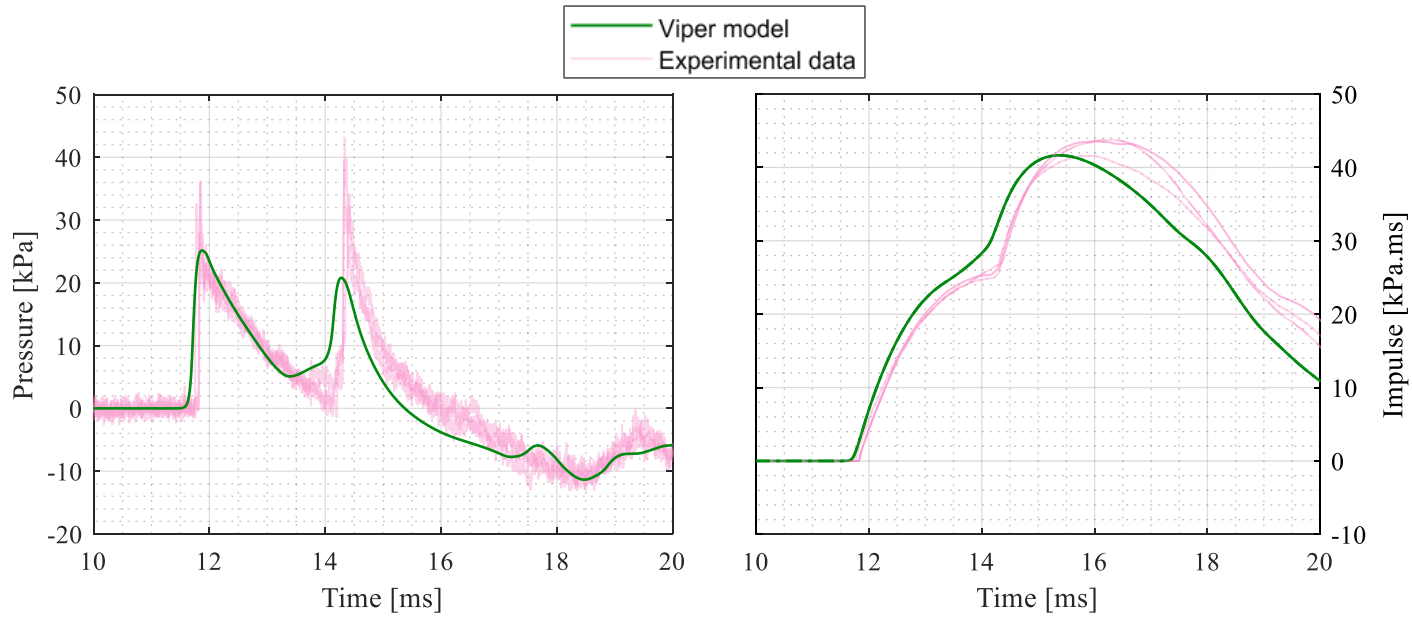

Figure 10: Viper Blast and experimental measurements of Pressure (left) and Impulse (right) vs Time for a cube charge at 6m standoff (8.9m/kg$^{1/3}$)

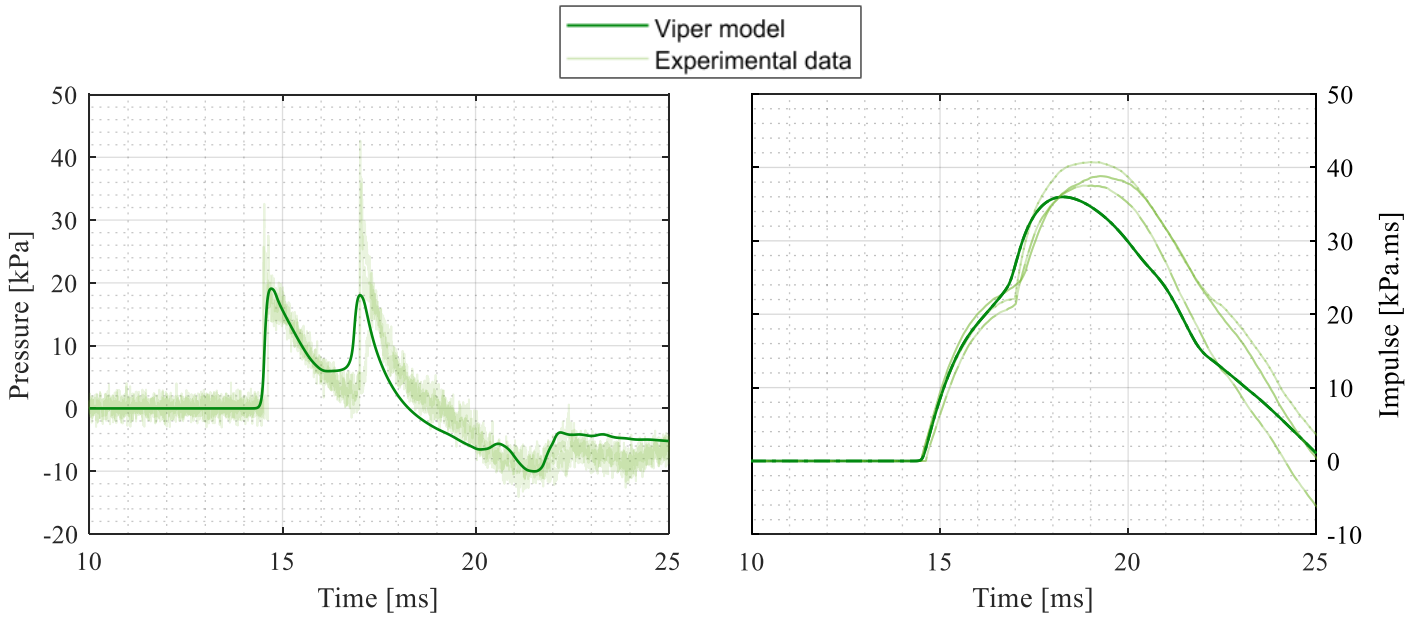

Figure 11: Viper Blast and experimental measurements of Pressure (left) and Impulse (right) vs Time for a cube charge at 7m standoff (10.4m/kg$^{1/3}$)

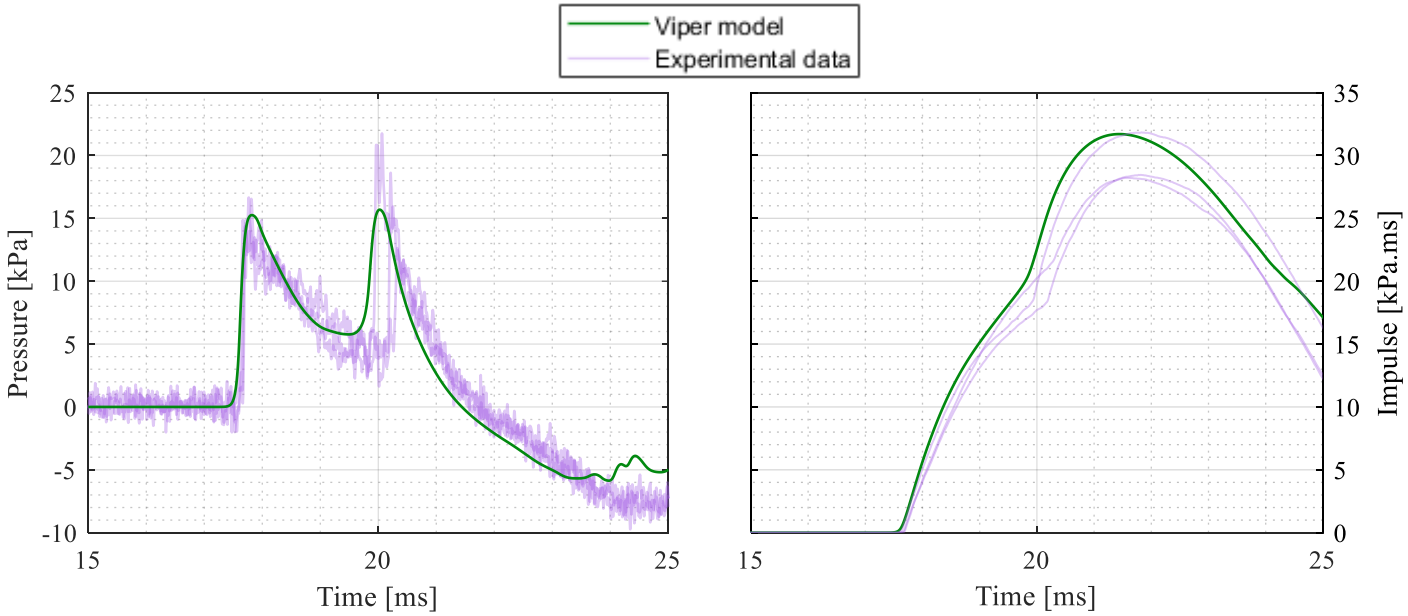

Figure 12: Viper Blast and experimental measurements of Pressure (left) and Impulse (right) vs Time for a cube charge at 8m standoff (11.9m/kg$^{1/3}$)

Looking at the impulse, Viper again offers very reasonable predictions of the overall shape of the impulse-time curve, with both Viper and the experimental data following the same curve. There is a tendency toward slight overprediction during the primary and subsequent shocks, before the point of peak impulse, after which Viper underpredicts impulse, a result of the early and under-prediction of the subsequent shock. Viper's smoothing of the additional shock due to the mesh resolution also contributes to this underprediction by artificially inflating the impulse as it neglects the drop in pressure before the arrival of the subsequent shock.

Viper predicts the shape of the subsequent shock curve well, with the model offering a good match to the experiments. However, it does generally underpredict the magnitude and arrival time of the shock: this can be improved by increasing the resolution of the mesh [34].

DISCUSSION

Pressure

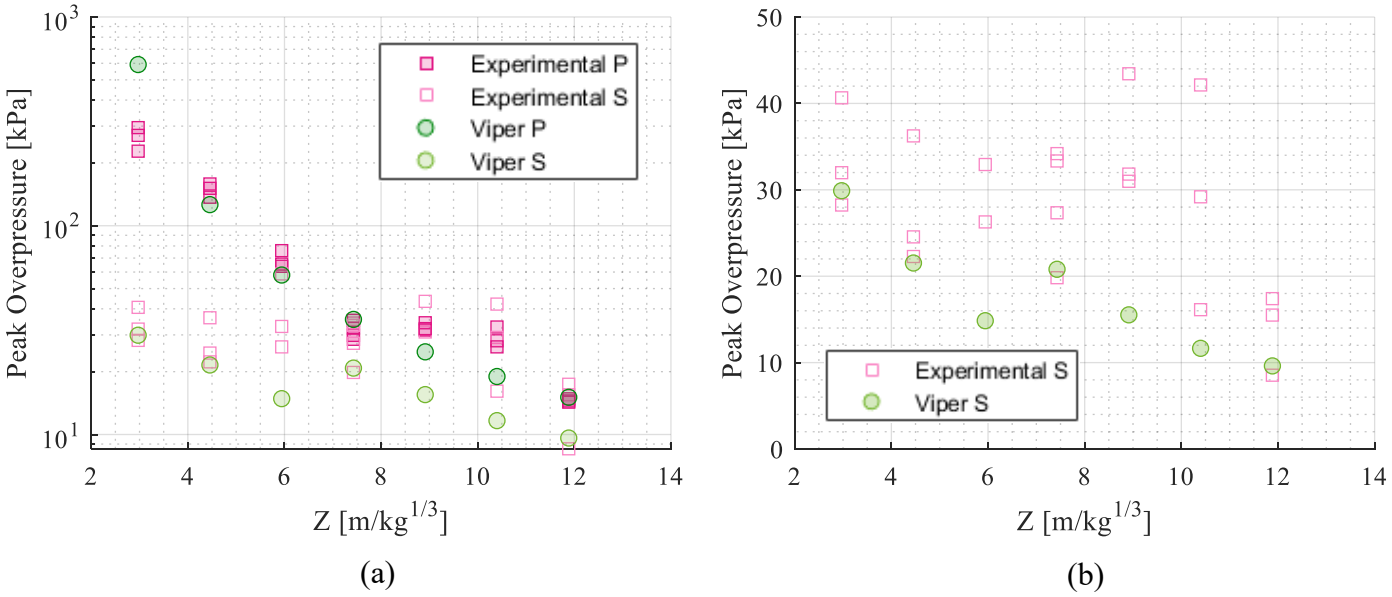

Figure 13: (a) Viper Blast model and experimental Peak overpressure vs Scaled distance for both Primary and subsequent shock and (b) Subsequent shock only. P and S denote Primary and Subsequent shock respectively.

Figure 13a shows both primary and subsequent shocks on a logarithmic scale, whereas 13b shows only the subsequent shock, on a linear scale.

Viper offers very reasonable predictions for the peak overpressure of the primary shock (Figure 13a), with the predicted values falling within 20kPa of the range of experimental values for most of the tested scaled distances. For the 3m/kg$^{1/3}$ scaled distance, the Viper model offers a significant overprediction, however this may be a result of experimental data rather than the model, as discussed earlier. Viper offers a slight underprediction for the 8.9 and 10.4m/kg$^{1/3}$ scaled distances; however it is still within 10kPa.

Figure 13b shows that, whilst there is generally a spread of ~10-15 kPa amongst the peak pressure of the subsequent shock at each respective scaled distance, the Viper model peak pressure falls within or ~5kPa from this range for most of the scaled distances. Viper tends towards underprediction for the subsequent shock peak overpressure, which is the authors believe to be related to the slightly early rise time seen in Figures 6-12 and 14. The additional variation in subsequent shock, especially as the scaled distance increases, is potentially due to the additional complication arising

from the interaction of the blast waves propagating further into free air. It is not yet known how uniform this behaviour is from charge to charge.

Arrival time

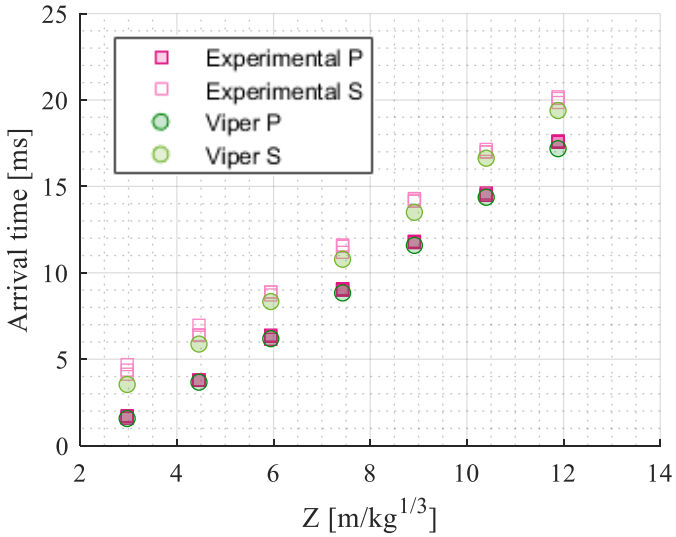

Figure 14: Viper Blast model and experimental Arrival time vs Scaled distance. P and S denote Primary and Subsequent shocks respectively.

Figure 14 shows the extracted arrival times of the primary and subsequent shocks for both Experimental data and Viper models. Time adjustments performed in previous sections to facilitate qualitative analysis have been reverted, and therefore the times are "as recorded". As can be seen, Viper offers very accurate predictions for the arrival time of the primary shock, within 0.4ms at all scaled distances. The prediction of the subsequent shock arrival is also very reasonable, with predictions within 1ms for all scaled distances. The subsequent shock predictions also appear to improve with increasing scaled distance, whereas the predictions for the primary shock are the opposite, i.e. more accurate at shorter scaled distances. For both shocks, the Viper predictions are consistently early, indicating that Viper is not fully capturing the stochastic nature of the detonation and early fireball expansion, wherein a complex multitude of overlapping waves with different wave speeds forms the subsequent shock.

Duration

Figure 15 shows the duration of the positive phase of the cube charge. The duration is calculated as the time between the arrival of the primary shock and the time at peak impulse. The whole waveform is considered here, hence the lack of P and S distinction. Viper provides a reasonably consistent underprediction of <0.6ms at all standoff distances. At these latter scaled distances, there is more significant spread in the data- a result of the additional complications caused by the subsequent shock, contributing to the slight underprediction by Viper.

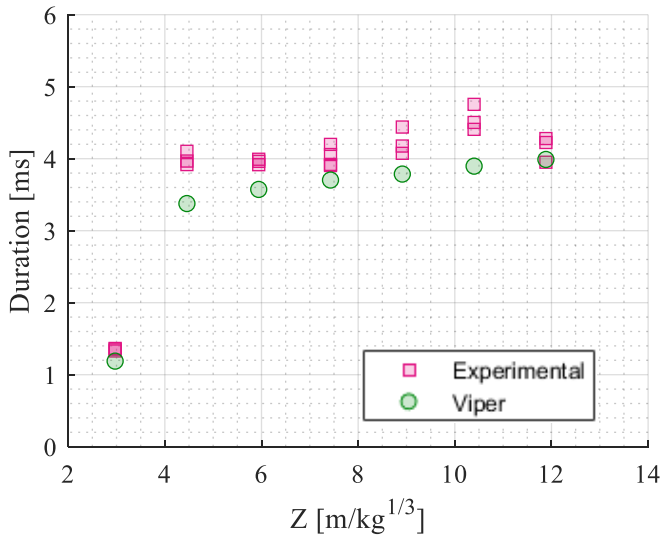

Figure 15: Viper Blast model and experimental Duration vs Scaled distance.

Impulse

Figure 16 shows the impulse of the waveform, here considered to be the total impulse contained between the time of arrival of the primary shock and the time of peak impulse. Similar to Figure 15, the whole waveform is considered here, so there are no P or S distinctions. For the latter standoff distances, Viper offers very reasonable predictions, with an overprediction within 10kpa for the latter 6 scaled distances. At a scaled distance of 3m/kg$^{1/3}$, Viper offers a significant overprediction of ~55kPa.ms however, as discussed earlier, this may be a feature of the experimental data rather than a fault of Viper, and therefore needs to be investigated further.

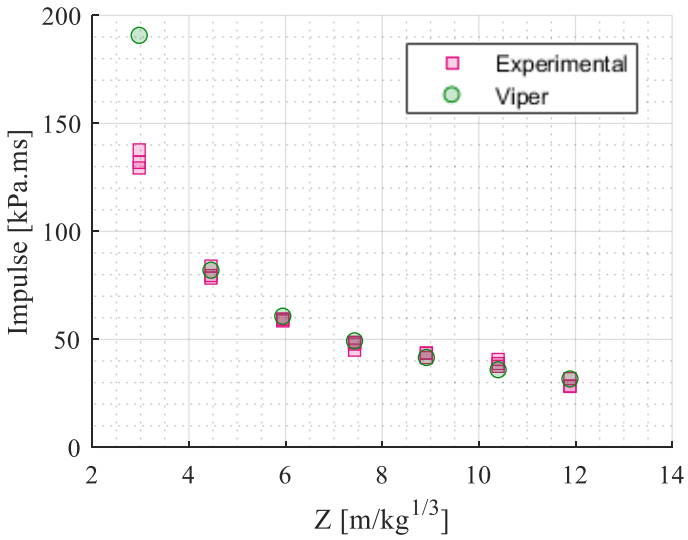

Figure 16: Viper Blast model and experimental Impulse vs Scaled distance.

Angle of propagation

Whilst this paper has focussed mainly on cube charges wherein the flat face of the cube is orientated towards the gauge; it is worth noting that the cube shape of the charge has significant impact on the pressure distribution at different angles of propagation around the charge. Figure 17 shows a map of peak primary pressure from a set of floor-level (elevated by 1mm to avoid any issues with boundary interaction) incident gauges modelled in a QS domain in Viper. The setup of this domain was identical to the other models shown in this paper: the initial detonation was modelled out to 0.3m using a C4 charge at a cell size of 1mm, before being remapped into a larger, QS domain with a cell size of 25 mm. The gauges were positioned between 0.3 and 8m, and 0 and 90° with radial and angular intervals of 0.05m and 1° respectively. The corner of the charge is aligned with the X=Y plane, illustrated by the grey line.

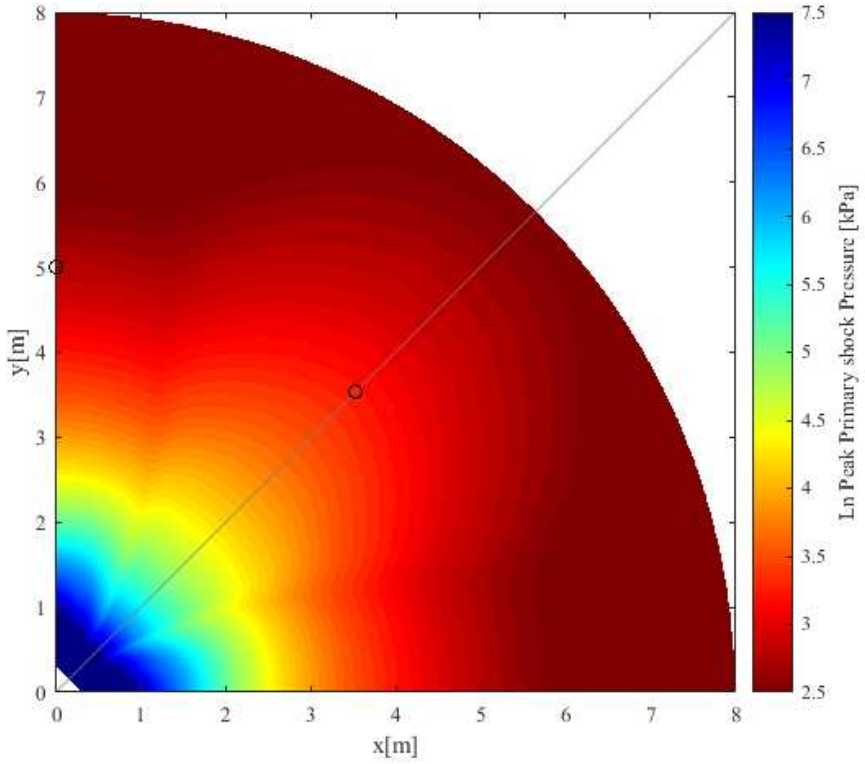

Figure 17: Peak primary shock pressure taken at an array of floor-level incident gauges, illustrating the change in pressure with at different angles of propagation on a logarithmic scale.

Figure 17 shows that the peak primary incident pressure varies significantly at different points around the charge, even at the same scaled distance. For example, at a standoff distance of 5m, the pressure increases from 17 kPa when aligned with the flat face of the cube, to 26 kPa when aligned with the corner of the charge. These points are shown on Figure 17 for clarity. Generally, the peak primary pressure at gauges aligned with the corner of the cube is higher than that of a gauge aligned with the flat face of the cube. There are also clear channels at ~ 30° from the flat faces, where the peak primary pressure is distinctly lower than other points at the same standoff distance.

CONCLUSION

This paper presents observations and discussion of the accuracy of the CFD solver Viper Blast when predicting the behaviour of blast waves from cube shape charges. It has already been established that cube charges exhibit an additional shock of significant magnitude, assumed to be a direct result of the change in mass distribution in a cube as opposed to a hemisphere. The subsequent shock develops with increasing scaled distance and has larger magnitude than the primary shock beyond 7.4m/kg$^{1/3}$. There is significant variation in the magnitude of the subsequent shock in some cases, likely a result of the complications in waveform as several waves overlap and coalesce. Also present clearly between 4.5 and 8.9m/kg$^{1/3}$ is a distinct additional wave, occurring between the primary and subsequent shocks, which decreases in magnitude from ~10kPa, so that by 10.4m/kg$^{1/3}$ the additional shock has fully merged with the subsequent shock.

Viper has shown it is very capable of predicting the overall waveform of a cube shape charge. It offers largely accurate representations of the pressure-time and impulse-time history curves at scaled distances 3-11kg/m$^{1/3}$. Viper captures the shape of both the primary and subsequent shocks with reasonable accuracy, also recognising the small additional wave which occurs between primary and subsequent shocks between 4.5 and 8.9m/kg$^{1/3}$. Moreover, it offers very accurate predictions of impulse and duration are predicted within 10kPa.ms and 0.6 respectively for all but one tested scaled distance. Viper also offers predictions accurate to within 0.4 and 1ms for the arrival time of the primary and subsequent shocks respectively. The peak pressure predictions are largely accurate, tending to fall within 20 and 5kPa of the experimental range for the primary and subsequent shocks respectively. Viper has also been used as a tool to show the variation in peak pressure at different angles of propagation around the cube charge, illustrating that higher pressures are observed when the gauge is in line with the corner of the cube, than when the gauge is aligned with a flat face.

Further research and testing is required to fully characterise the behaviour of cube shape charges at a wider range of standoff distances and angles of propagation. This can then be used to better inform and further improve predictive capabilities of CFD modelling tools such as Viper Blast.

ACKNOWLEDGEMENTS

This work forms part of a PhD project supported by ERDC under Contract No. W912HZ21C0036.

REFERENCES

[1] Kingery, C.N. and Bulmash, G. (1984) *Airblast parameters from TNT spherical air burst and hemispherical surface burst,* in *Technical Report ARBRL-TR-02555, U.S Army BRL, Aberdeen Proving Ground, MD, USA*

[2] Esparza, E.D. (1986). *Blast measurements and equivalency for spherical charges at small scaled distances,* in *International Journal of Impact Engineering*, *4*(1), pp.23-40.

[3] Rigby, S.E., Fuller, B. and Tyas, A. (2018) *Validation of near-field blast loading in LS-DYNA*, in *Proceedings of the 5th International Conference on Protective Structures*.

[4] U.S. DoD (Dept. of Defense) (2008) *Design of structures to resist the effects of accidental explosions,* in *Rep. No. UFC-3-340-02, Washington, DC*

[5] Randers-Pehrsons, G. and Bannister K.A. (1997) *Airblast Loading Model for DYNA 2D and DYNA 2D,* in *Technical Report ARL-TR-1310. Aberdeen Proving Ground, MD, USA.*

[6] Mendham, E.M., Rigby, S.E., Farrimond, D.G., Tyas, A and Pezzola, G., (2024) *Far field blast parameters from cuboidal charges* in *The 4th International Conference on Structural Safety under Fire and Blast Loading*, *London, UK*.

[7] Viper Applied Science, (2021). *Viper Blast. Stirling Simulation Services Limited: Aberdour, Scotland, UK*.

[8] Chester, A., Critchley, R. and Hazael, R (2025) *A comparison of far-field explosive loads by a selection of current and emerging blast software* in *International Journal of Protective Structures*, *16*(2), pp.387-418.

[9] Heylmun, J., Vonk, P. and Brewer, T (2019) Blastfoam theory and user guide. *Synthetik Applied Technologies: Austin, TX, USA*.

[10] ANSYS, I (1994) *Ansys autodyn, nonlinear dynamics analysis software*

[11] Dennis, A.A., and Rigby, S.E (2024) *The Direction-encoded Neural Network: A machine learning approach to rapidly predict blast loading in obstructed environments* in *International Journal of Protective Structures 15(3):*455-483

[12] Wisotski, J and Stoner, W (1965) *Characteristics of Blast Waves Obtained From Cylindrical High Explosive Charges*, *Denver Research Institute, Denver.*

[13] Wu, C., Fattori, G., Whittaker, A and Oehlers, D (2010), *Investigation of air-blast effects from spherical-and cylindrical-shaped charges* in *International Journal of Protective Structures*, *1(3),* pp.345-362.

[14] Plooster, M (1982), *Blast effects from cylindrical explosive charges: Experimental measurements.* Naval Weapons Center.

[15] Esparza, E (1992) *Spherical equivalency of cylindrical charges in free-air* in *25th Explosives Safety Seminar* (pp. 403-428).

[16] Garcia, S., Johnson, C., Joa, W. and McNeil, S (2019) *Investigation of Shock Propagation in Air from Sheet Explosive* in *International Society of Explosive Engineers.*

[17] Baker, W., Kulesz, J., Westine, P., Cox, P. and Wilbeck, J (1981) *A Manual for the Prediction of Blast and Fragment Loadings on Structures,* Department of Energy.

[18] Johnson, C., Mulligan, P., Williams, K., Langenderfer, M. and Heniff, J (2018) *Effect of explosive charge geometry on shock wave propagation* in *American Institute of Physics Conference Proceedings* Vol. 1979, No. 1.

[19] Williams, K., Langenderfer, M., Olbricht, G. and Johnson, C (2021) *Blast Wave Shaping by Altering Cross-Sectional Shape* in *Propellants, Explosives, Pyrotechnics*, *46(6*), pp.926-934.
[20] Vorobiev, O. and Ford, S (2025) *Airblast observations and near-field modelling of the large surface explosion coupling experiment* in *International Journal of Protective Structures*, *16*(2), pp.458-483.
[21] Rigby, S., Tyas, A., Bennett, T., Fay, S., Clarke, S. and Warren, J (2014) *A numerical investigation of blast loading and clearing on small targets* in *International Journal of Protective Structures, 5(3),* pp.253-274.
[22] Tyas, A. (2019). *Blast loading from high explosive detonation: what we know and what we don't kno*w in *13th International conference on shock and impact loads on structures, Guangzhou, China* (pp. 65-67).
[23] Netherton, M. D., Stewart, M. G., Buttenshaw, S. J., Reidy, K., & Rodgers, B. A. (2016) *Experimental data from the university of Newcastle's July 2014 repeatable explosive field trials, Technical Report.*
[24] Rigby, S. E., & Gitterman, Y. (2016). *Secondary shock delay measurements from explosive trials* in *Proceedings of the 24th Military Aspects of Blast and Shock*, *Halifax, Canada.*
[25] Bogosian, D., Yokota, M. and Rigby, S.E (2016) *TNT equivalence of C-4 and PE4: A review of traditional sources and recent data* in *Proceedings of the 24th military aspects of blast and shock*.
[26] Lee, E.L., Hornig, H.C. and Kury, J.W (1968) *Adiabatic expansion of high explosive detonation products* (No. UCRL-50422). Univ. of California Radiation Lab. at Livermore, Livermore, CA, US.
[27] Dobratz, B.M. and Crawford, P.C (1985) *LLNL explosives handbook – properties of chemical explosives and explosive simulants* in *Technical Report UCRL 52997, Lawrence Livermore National Laboratory, University of California, CA, USA.*
[28] Rigby, S. E., Tyas, A., Bennett, T., Clarke, S. D., & Fay, S. D (2014) *The negative phase of the blast load* in *International Journal of Protective Structures*, *5*(1), 1-19.
[29] Farrimond, D. G., Rigby, S. E., Clarke, S. D., & Tyas, A (2022) *Time of arrival as a diagnostic for far-field high explosive blast waves* in *International Journal of Protective Structures*, *13(2),* 379-402.
[30] Friedlander, F (1946) *The diffraction of sound pulses: Diffraction by a semi-infinite plane* in *Proceedings of the Royal Society of London. Series A. Mathematical and Physical Sciences.*
[31] Rigby, S. E., Tyas, A., Fay, S. D., Clarke, S.D. and Warren, J.A (2014) *Validation of semi-empirical blast pressure predictions for far field explosions-is there inherent variability in blast wave parameters?* in *Proceedings of the 6th International Conference on Protection of Structures against Hazards*.
[32] Tyas, A., Warren, J.A., Bennett, T. and Fay, S (2011) *Prediction of clearing effects in far-field blast loading of finite targets* in *Shock Waves 21(2):* 111–119.
[33] Farrimond, D., Nicholson, A., Nowak, P., Tetlow, L., Dennis, A., Lodge, T., and Stirling, C. (2024) *Experimental validation of Viper underwater explosion CFD solver* in *Proceedings of The 19th International Symposium on Interaction of the Effects of Munitions with Structures (ISIEMS) Bonn, Germany*.
[34] Draganić, H., & Varevac, D. (2018) *Analysis of blast wave parameters depending on air mesh size* in *Shock and Vibration*, *2018*(1), 3157457.